Constraining the history of inflation from microwave background polarimetry and laser interferometry

Jerod Caligiuri, Arthur Kosowsky, William H. Kinney, and Naoki Seto

The History of Inflation from Microwave Background Polarimetry and Laser Interferometry

Jerod Caligiuri and Arthur Kosowsky

Department of Physics and Astronomy, University of Pittsburgh, Pittsburgh, PA 15260 USA and
Pittsburgh Particle Physics, Astrophysics, and Cosmology Center (PITT PACC), Pittsburgh, PA 15260 USA

William H. Kinney

Department of Physics, University at Buffalo, Buffalo, NY 14260 USA

Naoki Seto

Department of Physics and Astronomy, Kyoto University, Kyoto 606-8502 JAPAN
(Dated: March 4, 2015)

A period of inflation in the early Universe produces a nearly scale-invariant spectrum of gravitational waves over a huge range in wavelength. If the amplitude of this gravitational wave background is large enough to be detectable with microwave background polarization measurements, it will also be detectable directly with a space-based laser interferometer. Using a Monte Carlo sampling of inflation models, we demonstrate that the combination of these two measurements will strongly constrain the expansion history during inflation and the physical mechanism driving it.

I. INTRODUCTION

The pursuit of comsological B-mode microwave background polarization [1, 2] at large angular scales has seen a burst of attention in the past year since the BICEP2 experiment [3] announced the possibility of a detection in March 2014. Further investigation has revealed that the dominant source of this signal is actually galactic dust [4–7] rather than being cosmological in nature. This does not rule out the existance of cosmological B-modes, but it is now clear that detecting a cosmological B-mode signal at significantly lower amplitude than the BICEP2 signal requires better characterization of foreground polarization signals via multi-frequency measurements. If we ultimately measure a primordial B-mode signal, it may provide an otherwise unobtainable window into physics at extremely high energies and the evolution of the Universe during its earliest moments.

A period of exponential expansion in the early Universe, known as inflation, resolves several observational difficulties with the standard cosmological model (e.g., [8–17]). Such a period of expansion can be driven by some component with a nearly constant energy density, such as the potential energy of an effective scalar field (the "inflaton"). During this epoch, quantum fluctuations in the inflaton field are amplified into classical density perturbations which grow by gravitational instability into the structures visible in the Universe today. Likewise, quantum fluctuations in the tensor components of the inflating spacetime are amplified into a stochastic background of gravitational waves, with a nearly scale-invariant power spectrum and an amplitude depending on the energy scale of inflation. Once generated, these tensor perturbations propagate almost freely through the Universe, their wavelengths increased by the expansion of the Universe and their amplitudes decreased by the same factor once the wavelength comes inside the horizon.

The hallmark of an inflationary gravitational wave background is its extremely wide range in wavelengths, roughly from the scale of the horizon today down to terrestrial scales. If inflation occurred when the temperature of the Universe was around the Grand Unification scale of 10^{16} GeV, the gravitational wave background will produce a pattern of B-mode polarization large enough to be seen by upcoming experiments. Remarkably, an inflationary tensor perturbation signal of roughly this amplitude will likely also be detectable directly with future space-based laser interferometers [18–27]. Direct detection will probe wavelengths that are 15 orders of magnitude smaller than those inducing microwave background signals; measurements at these two scales span a large portion of the observable inflation epoch, and may therefore reveal the physical process driving inflation. Gravitational wave backgrounds of smaller amplitude are more difficult to detect at both cosmological and local scales.

A recent paper showed that an interferometric detection of the inflationary tensor signal will provide qualitatively new information about inflation, namely a precise measurement of any departure from a pure power-law spectrum [28]. If we can obtain information about inflation at widely varying scales, a natural question arises: ultimately, how well can the history of inflation, and the physics driving it, be determined? Here, we determineconstraints on the expansion history during inflation, as well as the corresponding effective potential governing the evolution of the inflaton, from future measurements at both microwave background and interferometer

scales. We use a Monte Carlo method to generate random inflation models with an initially slowly varying inflaton value (the so-called "slow roll" condition) at the time when perturbations on the scale of the horizon today are generated [29, 30] and which satisfy current measurements [7]. Of these models, only a very small fraction satisfy tensor amplitude constraints at the few percent level on both scales, and the resulting expansion histories during inflation are strongly constrained.

Other recent works use similar techniques to constrain inflation. Ref. [31] considers only microwave background measurements; our results show that the additional information from an interferometric detection greatly restricts the range of acceptable inflation models. Ref. [23] focused on detectability of tensor perturbations in specific models by interferometers of a given sensitivity. We extend this work to consider the generic features of inflation models satisfying a particular pair of B-mode polarization and interferometer measurements. Ref. [22] considered models with the largest interferometer signals. We also consider interferometer measurements with sufficient sensitivity to constrain both the amplitude and spectral index of tensor perturbations at local scales, providing additional ability to discriminate between inflationary expansion histories.

II. METHODS

We compute the dynamical history and resulting scalar and tensor perturbation spectra for random inflation models chosen via the technique of Monte Carlo inflation flow potential reconstruction [29, 30]. The dynamics of an inflation model can be written in terms of the value of an effective scalar field ϕ (the "inflaton") and its potential energy $V(\phi)$; inflation occurs when the energy density is dominated by the inflaton potential energy. The field ϕ will evolve towards the minimum of the potential as inflation progresses. It is convenient to use the value of the effective inflaton field ϕ during inflation as a time parameter; this can be done as long as ϕ evolves monotonically to smaller values. The Hubble parameter during inflation, $H \equiv (1/a)da/dt$ with $a(t)$ the scale factor, can be used to construct a hierarchy of "slow-roll parameters" [32]

$$
\begin{aligned}
\epsilon &\equiv \frac{m_{\rm Pl}^2}{4\pi}\left(\frac{H'(\phi)}{H(\phi)}\right)^2, \\
\sigma &\equiv \frac{m_{\rm Pl}}{\pi}\left[\frac{1}{2}\left(\frac{H''}{H}\right) - \left(\frac{H'}{H}\right)^2\right], \\
{}^{\ell}\lambda_{\rm H} &\equiv \left(\frac{m_{\rm Pl}^2}{4\pi}\right)^{\ell}\frac{(H')^{\ell-1}}{H^{\ell}}\frac{d^{(\ell+1)}H}{d\phi^{(\ell+1)}}, \qquad \ell \geq 2. \quad (1)
\end{aligned}
$$

where primes are derivatives with respect to ϕ and the Planck mass $m_{\rm Pl}$ sets the energy units. The evolution of the parameters during inflation is determined by a system

of first-order linear equations [29, 33],

$$
\begin{aligned}
\frac{d\epsilon}{dN} &= \epsilon\,(\sigma + 2\epsilon), \\
\frac{d\sigma}{dN} &= -5\epsilon\sigma - 12\epsilon^2 + 2\left({}^2\lambda_{\rm H}\right), \\
\frac{d\left({}^{\ell}\lambda_{\rm H}\right)}{dN} &= \left[\frac{\ell-1}{2}\sigma + (\ell-2)\,\epsilon\right]\left({}^{\ell}\lambda_{\rm H}\right) + {}^{\ell+1}\lambda_{\rm H}. \quad (2)
\end{aligned}
$$

In these equations the time variable is the number of expansion e-folds before the end of inflation $N \equiv \ln(a_{\rm end}/a)$ where

$$
\frac{d}{dN} = \frac{m_{\rm Pl}}{2\pi^{1/2}}\sqrt{\epsilon}\,\frac{d}{d\phi}. \quad (3)
$$

Given a solution for $\epsilon(\phi)$, $H(\phi)$ can be obtained from the definition of ϵ, which then requires normalization given the observed amplitude of the scalar power spectrum [34]. The effective potential $V(\phi)$ then follows from the equation of motion for $H(\phi)$,

$$
H^2(\phi)\left[1 - \frac{1}{3}\epsilon(\phi)\right] = \frac{8\pi}{3m_{\rm Pl}^2}V(\phi). \quad (4)
$$

Particular models of inflation are obtained by choosing initial values for the slow-roll parameters; their dynamical evolution corresponds to some trajectory in the slow-roll parameter space. In practice, we truncate the hierarchy Eqs. (2) above $\ell = 8$ (corresponding to a restricted subset of exact inflation models) and then evolve the evolution equations until inflation ends, which we take as the condition $\epsilon = 1$. Once the slow-roll parameters are all determined throughout inflation as a function of N, the primordial comoving curvature perturbation $\delta\rho/\rho$ arising from the scalar perturbations and the tensor/scalar ratio r are, to second-order in the slow roll parameters, given by [32, 35],

$$
\begin{aligned}
\frac{\delta\rho}{\rho} &\simeq \frac{H}{2\pi m_{\rm Pl}\sqrt{\epsilon}}, \\
r &\simeq 16\epsilon\left[1 - C\,(\sigma + 2\epsilon)\right] \quad (5)
\end{aligned}
$$

with $C \equiv 4(\ln 2 + \gamma) - 5 = 0.0814514$, where $\gamma \simeq 0.577$ is Euler's constant, and using the WMAP normalization convention for r [36]. Then the perturbation amplitudes as a function of N can be converted to amplitudes as a function of comoving wavenumber k at the end of inflation by the relation $a(N)H(N) = k$. Generating scalar and tensor perturbations for a random sampling of inflation models is thus reduced to choosing random initial points in the slow-roll parameter space. The resulting primordial scalar perturbation power spectrum $P(k) \simeq A_S(k/k_0)^{n_{\rm S}-1}$ and tensor power spectrum $P_T(k) \simeq A_T(k/k_0)^{n_{\rm T}}$ are both approximate power laws on cosmological scales around $k_0 = 0.05$ Mpc^{-1}, with $r \equiv A_T/A_S$.

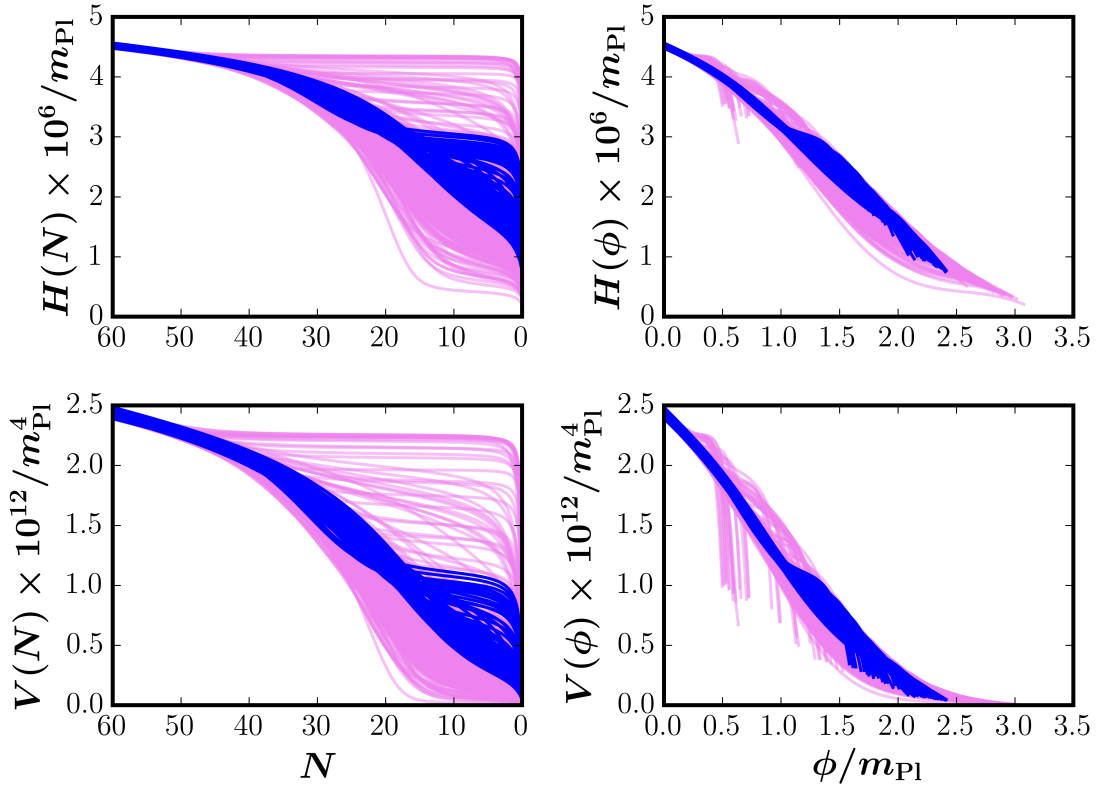We initially generate 2×10^4 models within an ellipsoidal parameter space region with principal axes $0.952 <$

FIG. 1: The expansion rates in the form of the Hubble parameter, H, and the effective potentials driving the evolution of the expansion, V, are shown. All models consistent with $r = 0.05 \pm 0.001$ at cosmological scales are plotted in violet. Those models that are also consistent at local scales with $\Omega_{\mathrm{GW}}(k_0 = 1.6 \times 10^{14}\mathrm{Mpc}^{-1}) = (8.2 \pm 0.69) \times 10^{-17}$ are plotted in blue. Note that modes with wave number $k = 1.6 \times 10^{14}\mathrm{Mpc}^{-1}$ correspond to frequencies $f = 0.25$ Hz. *Right Column*: H and V as a function of the number of efoldings before the end of inflation in the top and bottom panels respectively. *Right Column*: H and V as a function of the effective scalar field, ϕ driving inflation in the top and bottom panels respectively.

sitivy scaled by $u = 1/5$ at this fiducial amplitude) are displayed in Fig. 1 in blue. This additional local scale constraint reduces the number of allowed models to 93, 16% of those consistent with the future cosmological constraints and 0.5% of those consistent with current measurements.

Qualitatively, all models consistent with constraints at cosmological and local scales show similar behavior, as illustrated by the blue curves in the left panels in Fig. 1 between $N = 60$ and $N = 20$. A slight increase in the range of model behavior can be seen for $40 > N > 20$, which then translates to a widening of possibilities toward the end of inflation when the fields are departing from slow-roll conditions. Without intermediate and late inflationary epoch constraints on the tensor spectral amplitudes, we can identify properties of the local scale spectrum in order to further constrain the family of models permissible by observation. Specifically, the variety of allowable model amplitudes during intermediate and late time inflationary epochs will also reveal a distribution of spectral tilts, n_T, at local scales. For example, the blue curves in

Fig. 1, demonstrate a distribution of spectral tilts, n_T, for modes with wave numbers of $k = 1.6 \times 10^{14}\mathrm{Mpc}^{-1}$ that exited the horizon 20 efoldings before inflation ended. This distribution is shown in Fig. 2.

A group of allowed models are clustered around spectral tilts of $n_T = -0.06$ at local scales. The tail in the distribution toward higher values of n_T is easily associated with the models in Fig. 1 that fall more rapidly during intermediate epochs and then require a plateauing behavior in order to satisfy the required number of efoldings of expansion. These models all lie below the simpler main group of curves during intermediate times and above toward the end of inflation. These outlying models can be ruled out if interferometric measurements obtained sensitivity levels to constrain the tilt to $n_T = -0.06 \pm 0.02$ or better. In order to achieve these constraints at 95% confidence, the previously discussed DECIGO experiment will need a sensitivity level scaling parameter $u = 1/25$, an additional factor of 5 below the strain sensitivity (or a factor of 25 below the sensitivity to Ω_{GW}) used above ($u = 1/5$). This is a factor of 625 increase in sensitivity
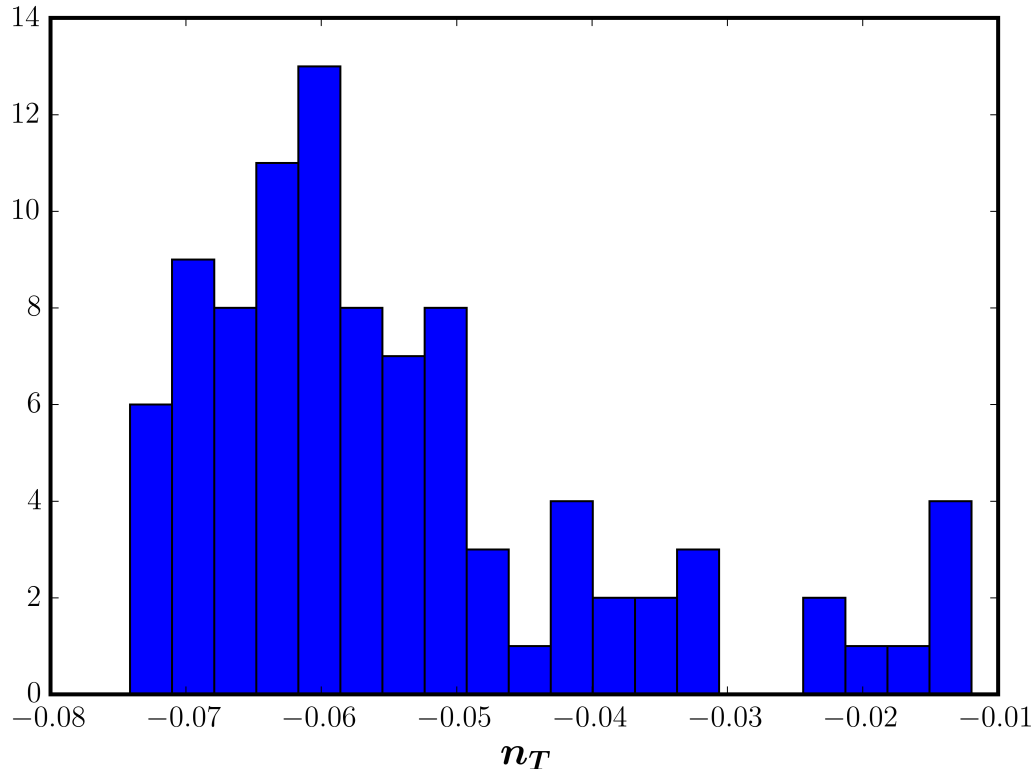
FIG. 2: The distribution of spectral tilts of models consistent with cosmological constraints with amplitudes corresponding to $r = 0.05 \pm 0.001$ and at local scales with $\Omega_{\mathrm{GW}} = (8.2 \pm 0.69) \times 10^{-17}$ at 95% confidence for modes with wavenumber $k = 1.6 \times 10^{14} Mpc^{-1}$ that exited the horizon 20 efoldings before the end of inflation.

to Ω_{GW} beyond the base design for DECIGO.

Applying these spectral tilt constraints to the models consistent at both cosmological and local scales as shown in blue in Fig. 1 (albeit without constricting the constraints on local scale amplitudes), we further reduce the number of consistent models to 78. This subset is illustrated in Fig. 3 in black, plotted over the models shown in Fig. 1. To further illustrate the distribution of each of these subsets of models, Fig. 4 indicates the mean and the band containing 95% of the models about the mean for each family of curves shown in Fig. 3. Here, the blue curves from Fig. 3 have their mean plotted as blue and the 95% spread of models shown as gray. Similarly for the violet curves from Fig. 3, the mean and 95% spread of models about the mean are shown in Fig. 4 as black and violet respectively. Although this additional constraint has not greatly reduced the number of allowed models,it has significantly restricted the qualitative form of the permissible models. If the local scale spectral index were measured to be $n_T = -0.02 \pm 0.02$, only a few models with more complex potential shapes would be consistent.

This conclusion will hold even for a tensor spectrum with a lower amplitude than the fiducially chosen value, provided that the amplitude can still be measured on both scales with similar fractional errors as used here. Of course, the lower the amplitude, the more technically challenging these measurements become. For amplitudes significantly below $r = 10^{-3}$, confusion with the residual gravitational lensing signal will prevent measurement of the tensor amplitude using B-mode polarization [47, 48], while the binary confusion limit becomes an increasing problem for interferometer measurements.

IV. DISCUSSION

These results clearly demonstrate the capacity of combined measurements of the tensor power spectrum at both microwave background and interferometric scales to constrain the history and physics of inflation. The family of inflation models consistent with both measurements is vastly restricted compared to inflation models consistent only with an amplitude measurement at a single scale. Furthermore, the combined measurements determine the inflaton potential and expansion history over
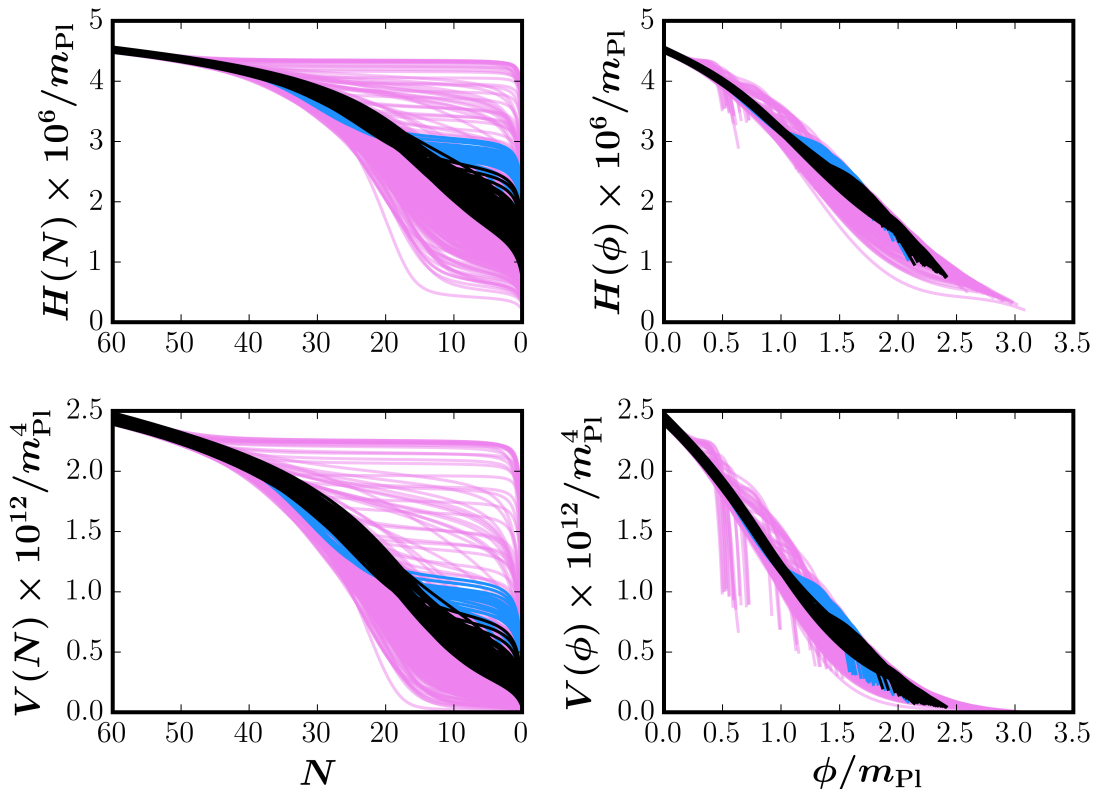
FIG. 3: The same models as shown in Fig. 1. The smaller subset of models that have local scale tensor spectral tilts of $n_{\mathrm{T}} \in [-0.08, -0.04]$ are plotted in black.

a wide range of field values and evolutionary epochs. We have assumed B-mode polarization measurements of the tensor amplitude with precision at the $r = 0.001$ level; upcoming polarization experiments with increased sensitivity and frequency coverage are expected to surpass this (see, e.g., [49]). We also assume a future interferometer measurement of the tensor amplitude at the 8% level, which will be challenging but feasible if there is in fact a measureable cosmological tensor signal. Pushing the sensitivity of interferometric experiments farther opens the possibilty of further restricting the family of allowed models via the tilt of the spectra at these scales. Clearly such a measurement vastly restricts the behavioral variety of consistent inflationary models.

It may seem surprising that the tilt of the tensor spectrum varies so greatly between scales corresponding to 60 and 20 efoldings before the end of inflation. Recall, however, that during slow-roll $\epsilon \propto (V'/V)^2$, where the prime indicates the derivative with respect to the effective scalar field ϕ and V is the effective potential of that scalar field. As illustrated in Fig. 1 and 3, the potentials drop by a factor of approximately 3 between $N = 60$ and $N = 20$. When plotted as a function of ϕ, this roughly corresponds to the interval of $\phi/m_{\mathrm{Pl}} \in [0.0, 1.0]$. In this

interval, the slope of the potential steepens only slightly. Taking both the slight steepening of the slope and the drop in the value of the potential into consideration, we estimate epsilon to increase by a factor of *at least* 9. Our fiducial selection of models at $N = 60$ have amplitudes corresponding to $r = 0.05 \pm 0.001$ and have tilts centered on $n_{\mathrm{T}} = -6.25 \times 10^{-3}$ (as to be expected according to the slow-roll consistency relation, $r = -8n_{\mathrm{T}}$). Moving to $N = 20$ and increasing ϵ by a factor of roughly 9 then results in a distribution of tilts at these scales to be centered on roughly $n_{\mathrm{T}} \approx -0.06$. This is consistent with what we have found in the distribution of tilts at local scales, as illustrated in Fig. 2, and is indicative of the dominance of slow-roll behavior throughout these 40 efoldings of evolution. The outlying models underwent brief departures from slow-roll evolution before returning to ensure the necessary number of efoldings of expansion are completed. This behavior directly translates to the tilt of the spectrum at local scales, thus providing a probe of the expansion history and effective potential driving inflation during epochs corresponding to otherwise unmeasureable scales.

We have made the simplifying physical assumption that reheating after inflation happens quickly, i.e. on
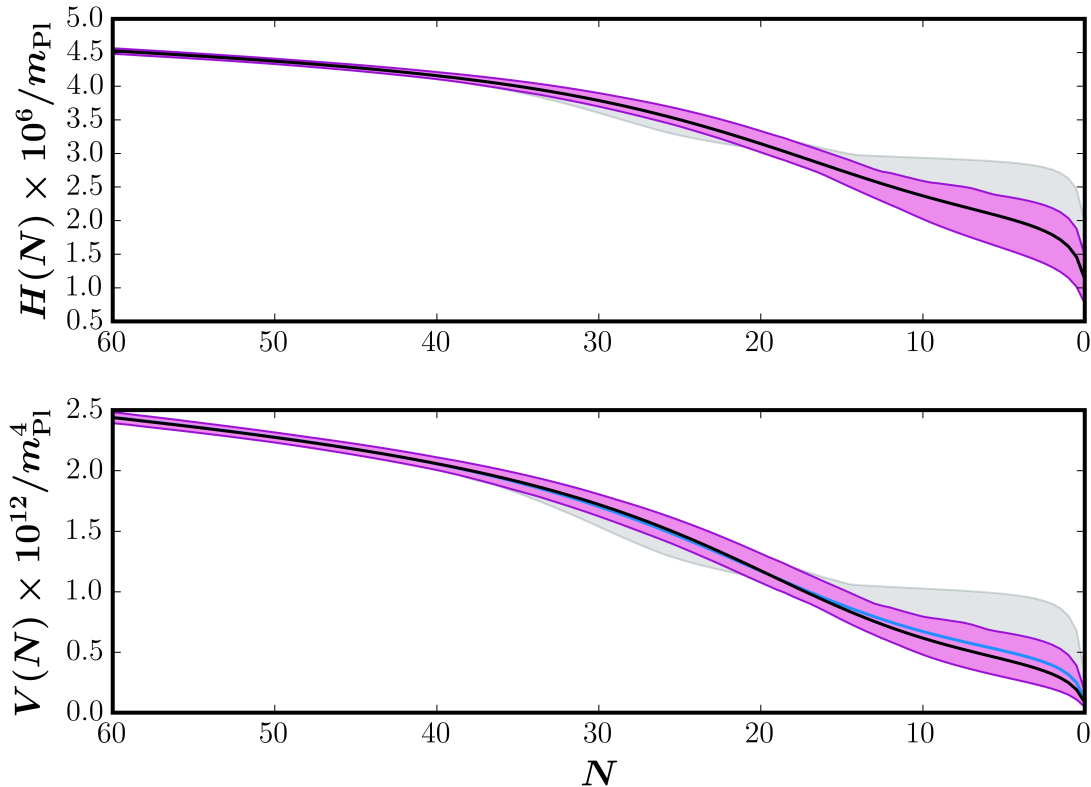
FIG. 4: The mean and 95% spread about the mean of models shown in Fig. 3. Here the potentials and expansion rates consistent with $r = 0.05 \pm 0.001$ with 2σ confidence at cosmological scales (corresponding to 60 efoldings before the end of inflation), as well as at local scales (corresponding to 20 efoldings before the end of inflation) with $8\%, 2\sigma$ error on the amplitude have their mean plotted in blue and the spread of models illustrated as a gray band. The set of models that additionally have spectral tilt constraints at local scales in the range of $-0.08 < n_{\rm T} < -0.04$ have their mean plotted in black with their spread about the mean as a violet band.

a time scale less than a Hubble time, so it has little effect on the expansion history of the Universe. Some models of reheating take significantly longer than this, resulting in a period of matter-dominated expansion prior to the usual radiation-dominated era which can modify the tensor amplitude at small scales (e.g., [50]). Measurements of both the tensor amplitude and the scalar spectral index will give interesting constraints on the duration of any reheating epoch [51]. An extension of the present analysis to include reheating will be considered elsewhere.

The numerical analysis in this paper does not have a rigorous quantification of Monte Carlo coverage of the inflation model space. The truncation of the slow-roll hierarchy at a given order results in only a particular subset of inflation models in the allowed model space. Larger computational efforts can include higher-order truncations, effectively expanding the model space which is explored, and more total models in each Monte Carlo, which will sharpen statistical conclusions. It is unlikely that models not available in our 8th-order slow-roll hierarchy will change our conclusions in a qualitative sense,

since the allowed models span a wide range of potentials, as is visible in Fig. 1. However, whether rare successful models exist which are clearly different from the family of models identified here is an interesting open question. These rare cases may be further constrained by additional sources of information.

The results presented here show that a detection of inflationary tensor perturbations at two widely separated scales, the cosmological scale via B-polarization of the microwave background and the Earth-Moon scale via a space-based laser interferometer, will determine the dynamical history of the Universe during the inflation era. In turn, such measurements will give strong constraints on fundamental physics at energy scales of 10^{16} GeV, inaccessible by any other means.

---

[1] M. Kamionkowski, A. Kosowsky, and A. Stebbins, Phys.Rev. **D55**, 7368 (1997).

[2] M. Zaldarriaga and U. Seljak, Phys.Rev. **D55**, 1830 (1997).

[3] P. Ade et al. (BICEP2 Collaboration), Phys.Rev.Lett. **112**, 241101 (2014).

[4] R. Flauger, J. C. Hill, and D. N. Spergel, JCAP **1408** (2014).

[5] M. J. Mortonson and U. Seljak (2014), arXiv:1405.5857.

[6] Planck Collaboration, R. Adam, P. A. R. Ade, N. Aghanim, M. Arnaud, J. Aumont, C. Baccigalupi, A. J. Banday, R. B. Barreiro, J. G. Bartlett, et al. (2014), arXiv:1409.5738.

[7] BICEP2/Keck, Planck Collaborations, :, P. A. R. Ade, N. Aghanim, Z. Ahmed, R. W. Aikin, K. D. Alexander, M. Arnaud, J. Aumont, et al. (2015), arXiv:1502.00612.

[8] A. H. Guth, Phys.Rev. **D23**, 347 (1981).

[9] A. D. Linde, Phys.Lett. **B108**, 389 (1982).

[10] A. Albrecht and P. J. Steinhardt, Phys.Rev.Lett. **48**, 1220 (1982).

[11] D. Kazanas, Astrophys.J. **241**, L59 (1980).

[12] A. A. Starobinsky, Phys.Lett. **B91**, 99 (1980).

[13] K. Sato, Phys.Lett. **B99**, 66 (1981).

[14] K. Sato, Mon.Not.Roy.Astron.Soc. **195**, 467 (1981).

[15] V. F. Mukhanov and G. V. Chibisov, JETP Lett. **33**, 532 (1981).

[16] V. F. Mukhanov (2003), arXiv:astro-ph/0303077.

[17] A. D. Linde, Phys.Lett. **B129**, 177 (1983).

[18] M. S. Turner, Phys.Rev. **D55**, 435 (1997).

[19] C. Ungarelli, P. Corasaniti, R. Mercer, and A. Vecchio, Class.Quant.Grav. **22**, S955 (2005).

[20] A. Cooray, Mod.Phys.Lett. **A20**, 2503 (2005).

[21] T. L. Smith, M. Kamionkowski, and A. Cooray, Phys.Rev. **D73**, 023504 (2006).

[22] T. L. Smith, H. V. Peiris, and A. Cooray, Phys.Rev. **D73**, 123503 (2006).

[23] S. Chongchitnan and G. Efstathiou, Phys.Rev. **D73**, 083511 (2006).

[24] B. C. Friedman, A. Cooray, and A. Melchiorri, Phys.Rev. **D74**, 123509 (2006).

[25] S. Kuroyanagi, S. Tsujikawa, T. Chiba, and N. Sugiyama (2014), arXiv:1406.1369.

[26] R. Jinno, T. Moroi, and T. Takahashi (2014), arXiv:1406.1666.

[27] L. Boyle, K. M. Smith, C. Dvorkin, and N. Turok (2014), arXiv:1408.3129.

[28] J. Caligiuri and A. Kosowsky, Phys.Rev.Lett. **112**, 191302 (2014).

[29] W. H. Kinney, Phys.Rev. **D66**, 083508 (2002).

[30] R. Easther and W. H. Kinney, Phys.Rev. **D67**, 043511 (2003).

[31] C. R. Contaldi (2014).

[32] J. E. Lidsey, A. R. Liddle, E. W. Kolb, E. J. Copeland, T. Barreiro, et al., Rev.Mod.Phys. **69**, 373 (1997).

[33] M. B. Hoffman and M. S. Turner, Phys.Rev. **D64**, 023506 (2001).

[34] P. Ade et al. (Planck), Astron.Astrophys. **571**, A16 (2014).

[35] E. D. Stewart and D. H. Lyth, Phys.Lett. **B302**, 171 (1993).

[36] D. Spergel et al. (WMAP Collaboration), Astrophys.J.Suppl. **148**, 175 (2003).

[37] C. Bennett et al. (WMAP), Astrophys.J.Suppl. **208**, 20 (2013).

[38] C. P. Ahn et al. (SDSS Collaboration), Astrophys.J.Suppl. **203**, 21 (2012).

[39] D. H. Jones, M. A. Read, W. Saunders, M. Colless, T. Jarrett, et al. (2009), arXiv:0903.5451.

[40] C. Blake, E. Kazin, F. Beutler, T. Davis, D. Parkinson, et al., Mon.Not.Roy.Astron.Soc. **418**, 1707 (2011).

[41] K. Freese and W. H. Kinney (2014), arXiv:1403.5277.

[42] P. Ade et al. (Planck) (2015), 1502.01589.

[43] T. L. Smith, M. Kamionkowski, and A. Cooray, Phys.Rev. **D78**, 083525 (2008).

[44] Y. Watanabe and E. Komatsu, Phys.Rev. **D73**, 123515 (2006).

[45] S. Weinberg, Phys.Rev. **D69**, 023503 (2004).

[46] S. Kawamura, T. Nakamura, M. Ando, N. Seto, K. Tsubono, et al., Class.Quant.Grav. **23**, S125 (2006).

[47] L. Knox and Y.-S. Song, Phys.Rev.Lett. **89**, 011303 (2002).

[48] C. M. Hirata and U. Seljak, Phys.Rev. **D68**, 083002 (2003).

[49] A. Kogut, D. Fixsen, D. Chuss, J. Dotson, E. Dwek, et al., JCAP **1107**, 025 (2011).

[50] S. Kuroyanagi, T. Chiba, and N. Sugiyama, Phys.Rev. **D83**, 043514 (2011).

[51] L. Dai, M. Kamionkowski, and J. Wang, Phys.Rev.Lett. **113**, 041302 (2014).